Temperature dependence of the Ge(111) surface electronic structure probed by inelastic H atom scattering

Kerstin Krüger [1], Nils Hertl [2,*], Alec M. Wodtke [1,2,3] and Oliver Bünermann [1,2,3,†]

[1] *Institute of Physical Chemistry, Georg-August University, 37077 Göttingen, Germany*

[2] *Department of Dynamics at Surfaces, Max-Planck-Institute for Multidisciplinary Sciences, 37077 Göttingen, Germany*

[3] *International Center of Advanced Studies of Energy Conversion, Georg-August University, 37077 Göttingen, Germany*

(Received 13 April 2023; revised 12 February 2024; accepted 28 February 2024; published 29 March 2024)

Experimental methods capable of determining the electronic properties of the surfaces of materials suffer from severe limitations, including interference from bulk electronic states, insensitivity to unoccupied states, and the requirement that the material be conducting. In this work, we introduce inelastic H atom scattering as a tool to probe the electronic structures of surfaces, which can be applied to both conducting and nonconducting samples while exhibiting exceptional surface sensitivity. We illustrate the method for the example of Ge(111). The measurements show a semiconducting surface at low temperature that continuously becomes increasingly metallic at high temperature.

DOI: 10.1103/PhysRevMaterials.8.034603

I. INTRODUCTION

A variety of methods has been devised to characterize the bulk electronic properties of semiconductor materials. For example, optical absorption-edge spectroscopy provides semiconductor band gaps [1–3] and photoelectron spectroscopy (PES) is one of the most powerful tools to probe the bulk electronic states of solids [4–6]. Extreme ultraviolet lithography used in the industrial manufacture of modern microelectronics now can produce transistor gates as small as 5 nm [7], only one order of magnitude larger than the van der Waals diameter of the silicon atom. Materials structured on this length scale possess as many—indeed, perhaps more—atoms at the surface than within the bulk. Hence, the properties of such devices will depend strongly on the nature of their surfaces, typically found at buried interfaces. Furthermore, we know from studies at exposed interfaces that the electronic properties of surface states do not necessarily reflect those of the bulk—the famous Si(111)(7×7) surface, for instance, is metallic, while Si is a bulk semiconductor [8].

The methods currently available are limited when probing surface electronic states. PES is not, strictly speaking, surface selective as photoelectrons originating from several atomic layers below the surface contribute to the signals. PES spectra therefore include information about bulk and surface states [4] and distinguishing between them can be a challenge. Furthermore, conventional PES is sensitive only to occupied electronic states. Electron-energy-loss spectroscopy (EELS) is an alternative to study electronic surface states [9] even though it is typically used only to study surface phonons and adsorbate vibrations [10]. It is indeed more surface sensitive than PES, when low-energy incidence electrons are used. Unfortunately, the desired signals may be buried under signals from near-elastic electron scattering, which often dominate the spectrum in the area of interest [11]. Scanning tunneling spectroscopy (STS) is another approach to obtaining information about electronic surface states [12], even providing in favorable cases the spatial properties of the surface states. However, the strong electric fields near the tip can alter the material's electronic states, a complicating effect referred to as tip-induced band bending [13]. We note that all of these methods are limited to analysis of conducting materials.

In order to achieve enhanced surface sensitivity, metastable rare-gas atoms have been used to generate exoelectrons, whose energy spectrum can be analyzed just as in PES [14–16]. In this type of "metastable atom electron spectroscopy" (MAES), interpreting the spectra may be complicated by the need to identify the metastable quenching mechanism, of which two are commonly seen: Auger deactivation and the resonance ionization followed by Auger neutralization. A good example of the strengths and weaknesses of MAES when applied to semiconductor surfaces can be found in Ref. [17].

It is interesting to realize that the surface sensitivity of MAES arises from the fact that the atom is unlikely to penetrate the surface before being quenched. This suggests that other atom-scattering processes might be equally surface sensitive. In this work, we apply this insight by using neutral beams of H atoms with tunable and nearly monochromatic energies. These atoms are scattered from the surface of the sample and we measure the translational inelasticity [18]. Remarkably, the light mass of H atoms often favors electronic over phononic excitation; hence, their translational inelasticity is qualitatively different for metal [19], insulator [20], and

*Present address: Department of Chemistry, University of Warwick, Coventry CV4 7AL, United Kingdom.

†Corresponding author: oliver.buenermann@chemie.uni-goettingen.de

semiconducting [21,22] surfaces. H atom scattering also offers the advantage of being exquisitely surface specific; this is due to the fact that atoms that penetrate the surface are, for all practical purposes, guaranteed to remain adsorbed at or below the surface [19,20]. Hence, the detected atoms arise exclusively from collisions at the surface. Another remarkable feature of the method arises from the fact that H atoms are uncharged, making this approach equally applicable to conducting or nonconducting materials. Furthermore, H atoms are very low-energetic probes compared to other methods. Finally, because the method explicitly involves electronic transitions, information about both occupied and unoccupied electronic states can be obtained.

We illustrate the advantages of this approach showing experimental results on the temperature dependence of H atom inelasticity when scattering from Ge(111). At room temperature, Ge(111) exhibits a stable $c(2 \times 8)$ adatom surface reconstruction [23], the atomic geometry of which influences the nature of surface electronic states and leads to a surface with semiconducting properties [24–26]. As the temperature increases, the surface structure changes and at 573 K, the entire surface exhibits a disordered adatom arrangement, characterized by an apparent "(1×1)" diffraction pattern [27–29]. A second reversible transition is observed around 1050 K [30–32]. Previous work suggested a gradual metallization of the surface with increasing temperature that resulted in full surface metallization at 1050 K [33,34]. Using inelastic H atom scattering to follow these temperature-dependent electronic structure changes, we find three distinct components in the energy-loss distribution that can be assigned to the semiconducting and metallic behavior of the surface. The quantitative contribution of these three components can be easily determined between 138 and 1082 K. H atom scattering therefore represents a straightforward approach to obtaining the fundamental physical properties of a surface with complex electronic structure.

II. EXPERIMENTAL METHODS

The H atom scattering apparatus has been described in detail [18,35]. In short, a hydrogen atom beam with an incidence translational energy of $E_i = 0.99$ eV is formed by ultraviolet photodissociation of a supersonic molecular beam of hydrogen iodide using an excimer laser operating at 248 nm. A small portion of the H atoms passes through a skimmer and two differential pumping apertures, enters an ultrahigh-vacuum (UHV) chamber, and collides with a Ge crystal. The Ge sample is mounted on a five-axis manipulator, which allows the variation of the polar incidence angle ϑ_i with respect to the surface normal. The scattered H atoms are detected using Rydberg atom tagging time of flight (TOF) [36]. Here, the H atoms are excited to a long-lived Rydberg state just below the ionization limit and fly 250 mm, before they are field ionized and detected by a multichannel plate assembly. The detector is rotatable, enabling TOF distribution measurements at a variety of scattering angles ϑ_f. A multichannel scaler records the arrival time distribution. The time-of-flight distribution is converted to an energy-loss distribution applying the appropriate Jacobians. The surface temperature T_S can be adjusted between $\sim$140 and $\sim$1080 K using a liquid nitrogen flow cryostat combined with resistive heating. The temperature of the crystal was measured by a K-type thermocouple; temperatures above 450 K were calibrated using an external pyrometer. The Ge crystal used in this work was undoped, with a nominal purity of 99.999%. The Ge(111) surface was cleaned by cycles of Ar^+ ion sputtering and annealing at $\sim$950 K. Auger electron spectroscopy (AES) and low-energy electron diffraction were used to validate the cleanliness and $c(2 \times 8)$ structure of the room-temperature Ge(111) surface prior to experiments. Additional details about the sample can be found in the Supplemental Material [37]. We ensured that the energy-loss distributions did not change during the course of a measurement, to exclude any influence of the buildup of H coverage or other contaminations on the surface of the Ge(111) crystal during the measurement.

III. RESULTS

Figure 1 shows translational energy-loss distributions of H atoms scattered from a Ge(111) surface at surface temperatures of 138 K $< T_S <$ 1082 K. At 138 K, two well-separated features are visible. These features have been previously assigned to an electronically adiabatic scattering process at low energy losses and an electronically nonadiabatic process at high energy losses, where an electron is promoted from the valence band to the conduction band (VB-CB transition) of the surface, in total reflecting its semiconducting nature [21,22]. With increasing T_S, the intensity of these two features decreases and H atom flux at intermediate energy losses becomes increasingly apparent. In addition, the VB-CB transition shifts to lower energy as the surface band gap decreases with increasing T_S [34,38]. At $T_S = 1082$ K, the bimodal structure has completely vanished and a broad, featureless energy-loss distribution arises.

The energy-loss distribution at $T_S = 1082$ K is remarkably similar to those obtained for H atom scattering from metal surfaces [39]; consistent with previous work, this suggests that the surface of Ge(111) is metallic at high temperatures. To test this idea, we performed full-dimensional theoretical simulations of the H atom scattering from a copper surface using molecular dynamics with electronic friction (MDEF), which has been shown to accurately describe experimentally obtained H atom energy-loss distributions for metals [39]. We chose copper, as its mass (63.5 u) is closest to that of germanium (72.6 u) among the metals studied; hence, the phononic contribution to the H atom energy losses are similar in the two cases [39]. Details of the MDEF calculations appear in the Supplemental Material [37] (see also Refs. [40–45] therein).

Figure 2 shows that the H atom energy-loss distribution obtained with Ge(111) at $T_S = 1082$ K is nearly identical to the MDEF simulations of H scattering from Cu at $T_S = 950$ K. This strongly supports the hypothesis that the Ge(111) surface is metallic at high T_S, whereas it exhibits semiconducting behavior at low T_S.

To quantitatively determine the degree of metallicity at different temperatures, the energy-loss distributions of Fig. 1 were fitted to a three-component model—see Fig. 3. The

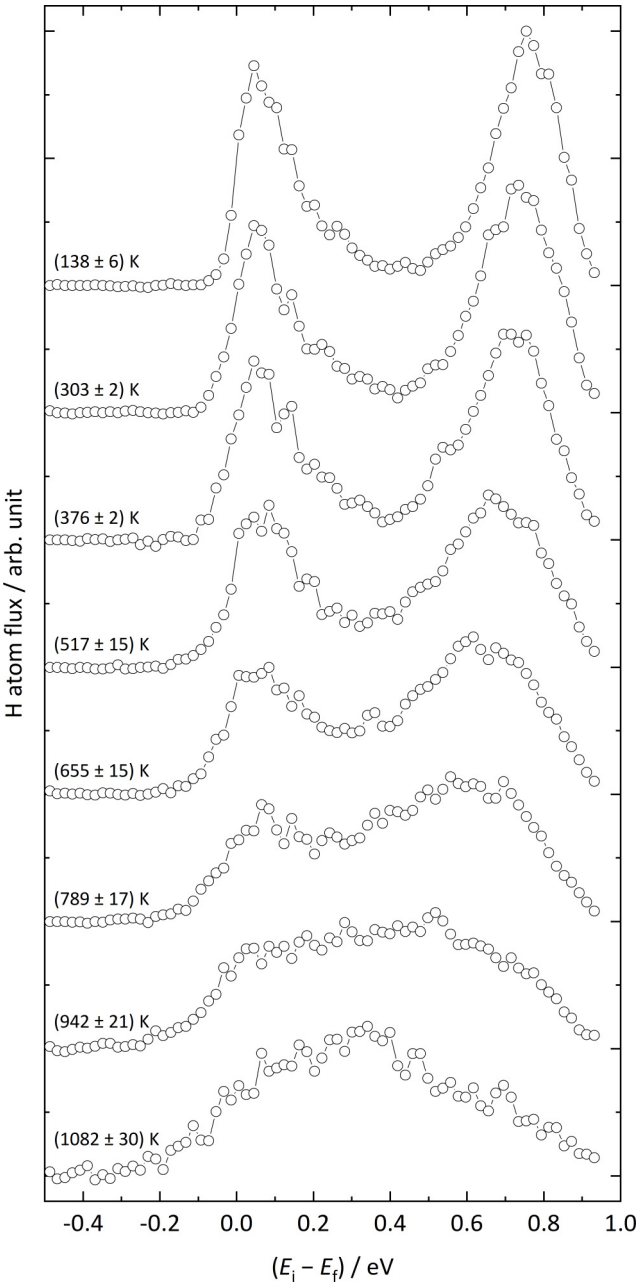

FIG. 1. Temperature-dependent energy-loss distributions for H atoms scattered from a Ge(111) surface. The polar incidence ϑ_i and scattering ϑ_f angles are both 45°. The energy-loss distributions are normalized to the integrated signal. The incident H atoms have a translational energy of $E_i = 0.99$ eV and travel along the [$\bar{1}$10] surface direction.

bimodal energy-loss distribution obtained at $T_S = 138$ K [Fig. 3(a)] exhibits two well-resolved features, characteristic of a semiconducting surface. In the following, the first, electronically adiabatic component, will be called S1, and the second component, corresponding to the nonadiabatic VB-CB transition, will be called S2. Both components were separately fitted to a sum of Gaussian functions. The energy-loss distribution obtained at $T_S = 1082$ K [Fig. 3(h)] was used to describe the metallic component, called M in the following, which grows in with increasing surface temperature. By varying the relative contributions of these three components, all six remaining energy-loss distributions could be fitted—see Figs. 3(b)–3(g). In this fitting, the shape and position of the S1 and M component were fixed, whereas the S2 component was allowed to broaden and shift with increasing T_S—this accounts for the reduction of the surface band gap with increasing surface temperature [34,38]. Additional details about the fit can be found in the Supplemental Material [37]. The three-component model results in an excellent fit to the data.

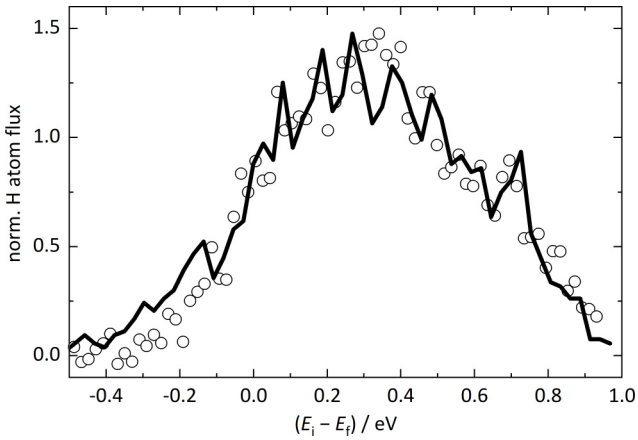

FIG. 2. Metallized surface of Ge(111) at elevated surface temperature. Inelastic H atom scattering data for Ge(111) at $T_S = 1082$ K (○) is compared to the results of MDEF simulations for Cu(111) at $T_S = 950$ K (black solid line). The H atoms travel along the [10$\bar{1}$] direction of the Cu(111) surface. The energy-loss distributions are normalized to the integrated signal. Conditions are otherwise the same as in Fig. 1.

Figure 4(a) shows the relative contribution of the semiconducting and metallic components vs T_S. The semiconductor components, S1 and S2, decrease, while the metallic contribution, M, increases with T_S. Above ∼800 K, the metallic contribution clearly dominates. The error bars of the relative intensities shown in Fig. 4(a) reflect the uncertainty of the fit due to the overlap of the S2 and M components. Errors of the surface temperature are primarily a result of the temperature calibration with an external pyrometer as the surface temperature measured with a thermocouple was found to be inaccurate at elevated temperatures of the crystal. Figure 4(b) shows the surface band gap as a function of surface temperature, determined from the onset of the S2 component in Fig. 3; for details see Supplemental Material [37]. This allows us to quantify the decrease of the surface band gap with increasing temperature.

IV. DISCUSSION

The results of this work complement previous studies using established methods [27–29,33,34,46–50]. Methods sensitive to structure have reported phase transitions in this temperature range. At room temperature, the semiconducting surface shows a c (2 × 8) structure [23]. With increasing temperature, a structural transition [27] was reported at 573 K as an

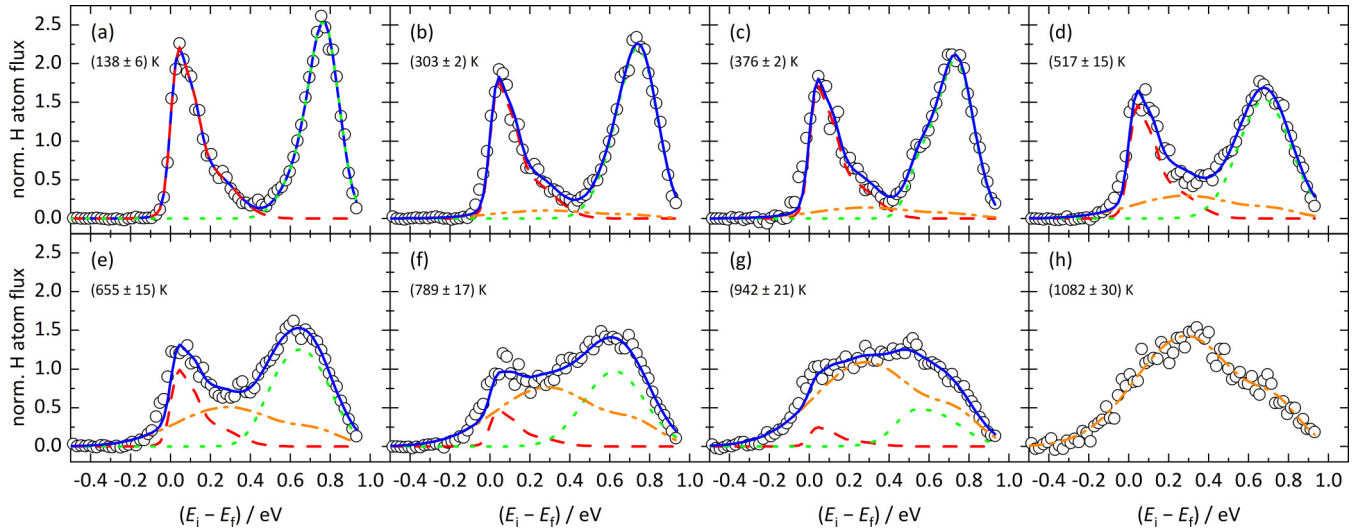

FIG. 3. Fit of the energy-loss distributions for H atoms scattered from Ge(111) at different surface temperatures with three components. Panels (a) to (h) show a fit of the energy-loss distributions (○) of H atoms scattered from Ge(111) at different surface temperatures, T_S. The data were fitted to a sum of three components (blue solid line): S1 (red dashed line), S2 (green dotted line), and M (orange dashed-dotted line). Details about the fit can be found in the text and the Supplemental Material [37]. The incidence translational energy is $E_i = 0.99$ eV, the polar incidence and scattering angles are $\vartheta_i = \vartheta_f = 45°$, and the incident H atoms travel along the $[\bar{1}10]$ surface direction.

apparent (1 × 1) diffraction pattern with weak half-order spots emerges that was attributed to the formation of an "incommensurate (2 × 2) surface structure" [28]. STM confirmed the existence of a disordered surface above 573 K; however; disordered regions were also seen at lower temperatures [29]. A reversible phase transition has also been reported at 1050 K [30–32].

No abrupt changes in the electronic structure that might be associated with a structural phase transition were observed in either PES [34,46,47] or EELS [50]. Instead, it was suggested that a gradual metallization of the surface takes place with increasing temperature [33,49]. The results of this work are clearly consistent with this suggestion—see Fig. 4. At the highest temperatures of this work (1082 K), the surface exhibits the inelasticity typical of a metal. Thus, our work confirms that the phase identified above 1050 K has the electronic properties of a metal. The first structural transition at 573 K is related to the adatoms becoming mobile on the surface. The adatoms are still present above the transition temperature but in a highly disordered arrangement with local short-range (2 × 2) order [28]. The 1:1 ratio of adatoms to rest atoms and the related electronic structure of the surface is preserved [47]. The nature of the structural transition at 1050 K is still under discussion. One model postulates a quasi-liquidlike, laterally diffusive metallic Ge surface bilayer due to incomplete surface melting, supported by experimental results from photoemission and photoabsorption spectroscopy [34] as well as medium-energy ion-scattering experiments [31]. However, a second model suggests a structurally well-defined surface that exhibits reduced surface corrugation. It is consistent with an ordered metallic solid state and supported by experimental results from helium atom scattering [32,51,52] and x-ray diffraction [53].

Our observations could be explained by a simple model where the populations of electrons in the surface conduction band and holes in the valence band both increase with temperature. This effect would be enhanced by the surface band gap's reduction with increasing temperature shown above [38]. These factors would permit H atom collisions to excite low-lying electron-hole pairs (EHP) in intraband transitions—the predominant energy-loss channel seen for metals—in both the surface valence and conduction bands, whereas at low temperatures, only interband excitations are possible. However, based on our observations, we cannot exclude a change in the electronic structure for temperatures above 1050 K. Within the uncertainties of our experiment, we are not able to conclude whether the metallic behavior is caused only by thermal population of the conduction band or additionally by a change of the surface electronic structure.

Our analysis also allows us to extract the temperature dependence of the surface band gap as shown in Fig. 4(b). The surface band gap decreases from a value of ∼0.5 eV at 138 K to ∼0.25 eV at 942 K. The value at low temperatures is in good agreement with STS measurements at 30 K that obtain a surface band gap of 0.49 eV [26]. The nearly linear decrease of the surface band gap by a factor of 2 in the studied temperature range is in correspondence to the temperature dependence of band gaps of bulk semiconductors [54] and the Ge(111)(2 × 1) semiconducting surface [38].

Finally, we want to emphasize that the physics of H atom inelasticity can be quantitatively simulated for both insulating and metallic surfaces using first-principles theory and validated dynamical models. In the case of metals, prior work has clearly shown that classical MDEF simulations

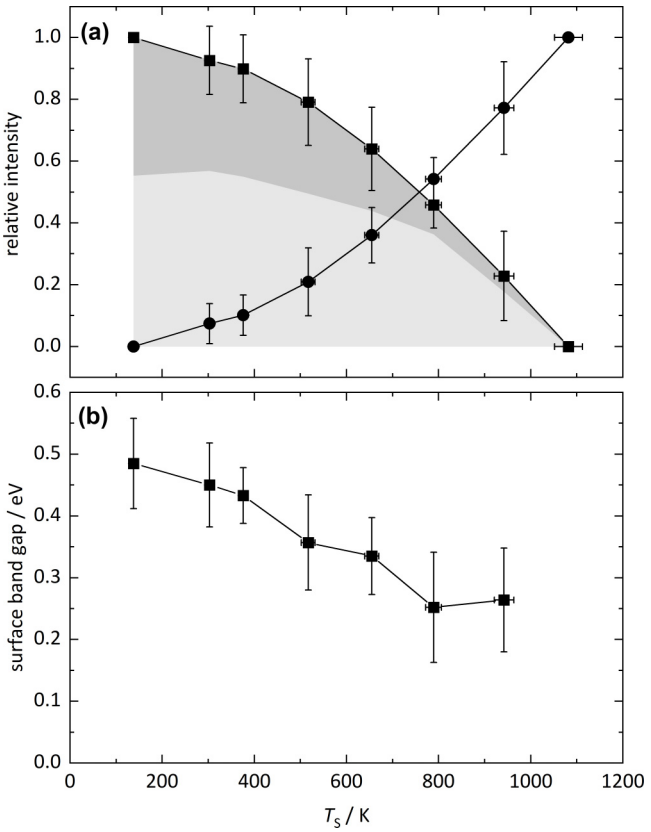

FIG. 4. Electronic character of the Ge(111) surface as a function of surface temperature. Panel (a) shows the relative intensities determined from the fits in Fig. 3 for the sum of the semiconducting components, S1+S2 (■) and the metallic component, M (•). Error bars reflect the uncertainty of the fit due to the overlap of the S2 and M components. Shaded areas correspond to the fractions of S1 (dark gray) and S2 (light gray) of the overall semiconductor component, respectively. Panel (b) shows the surface band gap as a function of surface temperature, determined from the onset of the S2 component in Fig. 3; for details see Supplemental Material [37]. In both panels, lines between data points are given as a guide to the eye.

employing high-dimensional potential-energy surfaces derived from density-functional theory data yield highly accurate energy-loss distributions [18,19,39]; here, the electronic friction picture is able to describe intraband EHP excitation induced by the H atom collision. Insulators, on the other hand, have a band gap with occupied states below the Fermi energy, and unoccupied states above the Fermi energy; hence, only interband electronic excitations are possible at low temperatures. Furthermore, the band gap is typically so large that energy can only be dissipated to phonons, meaning that H atom inelasticity can be quantitatively reproduced by molecular dynamics (MD) simulations within the Born-Oppenheimer approximation [20]. The ability to quantitatively model the H atom energy-loss spectra for two of the most common classes of surfaces simplifies its interpretation, allowing us to make conclusions about the temperature dependence of the electronic structure of Ge(111). The analysis needed to extract this information is remarkably simple. Inelastic H atom scattering has great potential to give detailed insights into the electronic properties of surfaces.

ACKNOWLEDGMENTS

We thank Alexander Kandratsenka, Yingqi Wang, and Hua Guo for helpful discussions. O.B. and A.M.W. acknowledge support from the Deutsche Forschungsgemeinschaft (DFG) under Grant No. 217133147 (SFB1073, project A04) and from the DFG, the Ministerium für Wissenschaft und Kultur, Niedersachsen and the Volkswagenstiftung under Grant No. 191331650. A.M.W. thanks the Max Planck Society for the advancement of science.

A.M.W. and O.B. conceived the project; O.B. supervised the experiment; K.K. performed the experiments; N.H. performed the MD simulations; K.K. analyzed the data; and K.K. and O.B. wrote the manuscript with feedback from A.M.W. and N.H.

The authors declare no competing interests.

[1] M. Becker and H. Y. Fan, Optical properties of semiconductors. III. Infra-Red transmission of silicon, Phys. Rev. **76**, 1531 (1949).

[2] G. W. Gobeli and H. Y. Fan, Infrared absorption and valence band in indium antimonide, Phys. Rev. **119**, 613 (1960).

[3] R. Zallen and M. P. Moret, The optical absorption edge of brookite TiO_2, Solid State Commun. **137**, 154 (2006).

[4] H. Y. Zhang, T. Pincelli, C. Jozwiak, T. Kondo, R. Ernstorfer, T. Sato, and S. Y. Zhou, Angle-resolved photoemission spectroscopy, Nat. Rev. Methods Primers **2**, 54 (2022).

[5] G. Schoenhense and H. J. Elmers, Spin- and time-resolved photoelectron spectroscopy and diffraction studies using time-of-flight momentum microscopes, J. Vac. Sci. Technol. A **40**, 020802 (2022).

[6] J. A. Sobota, Y. He, and Z. X. Shen, Angle-resolved photoemission studies of quantum materials, Rev. Mod. Phys. **93**, 025006 (2021).

[7] C. Vasilev, ASML's Cutting-Edge EUV Lithography Shrinks Transistors Down to 5 nm. AzoNano, https://www.azonano.com/article.aspx?ArticleID=5583 (2020).

[8] U. Backes and H. Ibach, Evidence for a 2d-metallic state of the clean 7 by 7 Si(111) surface, Solid State Commun. **40**, 575 (1981).

[9] M. Rocca, Low-Energy eels investigation of surface electronic excitations on metals, Surf. Sci. Rep. **22**, 1 (1995).

[10] A. Politano, On the fate of high-resolution electron energy loss spectroscopy (HREELS), a versatile probe to detect surface excitations: Will the Phoenix rise again?, Phys. Chem. Chem. Phys. **23**, 26061 (2021).

[11] M. Stöger-Pollach, H. Franco, P. Schattschneider, S. Lazar, B. Schaffer, W. Grogger, and H. W. Zandbergen, Cerenkov losses: A limit for bandgap determination and Kramers-Kronig analysis, Micron **37**, 396 (2006).

[12] R. M. Feenstra, Scanning tunneling spectroscopy, Surf. Sci. **299**, 965 (1994).

[13] R. M. Feenstra, A prospective: Quantitative scanning tunneling spectroscopy of semiconductor surfaces, Surf. Sci. **603**, 2841 (2009).

[14] S. Nannarone and L. Pasquali, Surface electronic properties by metastable deexcitation spectroscopy, Nucl. Instrum. Methods Phys. Res., Sect. B **182**, 227 (2001).

[15] Y. Harada, S. Masuda, and H. Ozaki, Electron spectroscopy using metastable atoms as probes for solid surfaces, Chem. Rev. **97**, 1897 (1997).

[16] F. Bozso, J. Arias, G. Hanrahan, R. M. Martin, J. T. Yates, and H. Metiu, Effect of surface electronic-structure on the deexcitation of He 2^1 S metastable atoms, Surf. Sci. **136**, 257 (1984).

[17] A. Ludviksson and R. M. Martin, *Mechanisms of Metastable Atom Quenching on GaAs(100)* (Springer, Berlin, 1993), pp. 238–243.

[18] O. Bünermann, A. Kandratsenka, and A. M. Wodtke, Inelastic scattering of H Atoms from surfaces, J. Phys. Chem. A **125**, 3059 (2021).

[19] O. Bünermann, H. Y. Jiang, Y. Dorenkamp, A. Kandratsenka, S. M. Janke, D. J. Auerbach, and A. M. Wodtke, Electron-hole pair excitation determines the mechanism of hydrogen atom adsorption, Science **350**, 1346 (2015).

[20] N. Hertl, A. Kandratsenka, O. Bünermann, and A. M. Wodtke, Multibounce and subsurface scattering of H atoms colliding with a van der Waals solid, J. Phys. Chem. A **125**, 5745 (2021).

[21] K. Krüger, Y. Wang, S. Tödter, F. Debbeler, A. Matveenko, N. Hertl, X. Zhou, B. Jiang, H. Guo, A. M. Wodtke, and O. Bünermann, Hydrogen atom collisions with a semiconductor efficiently promote electrons to the conduction band, Nat. Chem. **15**, 326 (2023).

[22] K. Krüger, Y. Q. Wang, L. J. Zhu, B. Jiang, H. Guo, A. M. Wodtke, and O. Bünermann, Isotope effect suggests site-specific nonadiabaticity on Ge(111)$c(2\times8)$, Nat. Sci. **4**, e20230019 (2024).

[23] D. J. Chadi and C. Chiang, New c-2×8 unit-cell for the Ge(111) surface, Phys. Rev. B **23**, 1843 (1981).

[24] R. S. Becker, B. S. Swartzentruber, J. S. Vickers, and T. Klitsner, Dimer-adatom-stacking-fault (DAS) and non-DAS (111) semiconductor surfaces: A comparison of Ge(111)-$c(2\times8)$ to Si(111)-(2×2), -(5×5), -(7×7), and -(9×9) with scanning tunneling microscopy, Phys. Rev. B **39**, 1633 (1989).

[25] F. J. Himpsel, Inverse photoemission from semiconductors, Surf. Sci. Rep. **12**, 3 (1990).

[26] R. M. Feenstra, J. Y. Lee, M. H. Kang, G. Meyer, and K. H. Rieder, Band gap of the Ge(111)$c(2\times8)$ surface by scanning tunneling spectroscopy, Phys. Rev. B **73**, 035310 (2006).

[27] P. W. Palmberg, Structure transformations on cleaved and annealed Ge(111) surfaces, Surf. Sci. **11**, 153 (1968).

[28] R. J. Phaneuf and M. B. Webb, A LEED study of Ge(111): A high-temperature incommensurate structure, Surf. Sci. **164**, 167 (1985).

[29] R. M. Feenstra, A. J. Slavin, G. A. Held, and M. A. Lutz, Surface diffusion and phase transition on the Ge(111) surface studied by scanning tunneling microscopy, Phys. Rev. Lett. **66**, 3257 (1991).

[30] E. G. McRae and R. A. Malic, A new phase transition at Ge(111) surface observed by low-energy-electron diffraction, Phys. Rev. Lett. **58**, 1437 (1987).

[31] A. W. Denier van der Gon, J. M. Gay, J. W. M. Frenken, and J. F. van der Veen, Order-disorder transitions at the Ge(111) surface, Surf. Sci. **241**, 335 (1991).

[32] C. A. Meli, E. F. Greene, G. Lange, and J. P. Toennies, Evidence for an order-order transition on the Ge(111) surface near 1050 K from high-resolution helium atom scattering experiments, Phys. Rev. Lett. **74**, 2054 (1995).

[33] S. Modesti, V. R. Dhanak, M. Sancrotti, A. Santoni, B. N. J. Persson, and E. Tosatti, High temperature surface metallization of Ge(111) detected by electron energy loss spectroscopy, Phys. Rev. Lett. **73**, 1951 (1994).

[34] A. Goldoni, A. Santoni, M. Sancrotti, V. R. Dhanak, and S. Modesti, Photoemission and photoabsorption study of the high-temperature phases of the Ge(111) surface, Surf. Sci. **382**, 336 (1997).

[35] O. Bünermann, H. Y. Jiang, Y. Dorenkamp, D. J. Auerbach, and A. M. Wodtke, An ultrahigh vacuum apparatus for H atom scattering from surfaces, Rev. Sci. Instrum. **89**, 094101 (2018).

[36] L. Schnieder, K. Seekamprahn, F. Liedeker, H. Steuwe, and K. H. Welge, Hydrogen-exchange reaction $H + D_2$ in crossed beams, Faraday Discuss. **91**, 259 (1991).

[37] See Supplemental Material at http://link.aps.org/supplemental/10.1103/PhysRevMaterials.8.034603 for additional details on the Ge(111) sample used; an extended explanation of the fitting procedure; and details of the molecular dynamics with electronic friction simulations.

[38] J. E. Demuth, R. Imbihl, and W. A. Thompson, Temperature-dependent electronic excitations of the Ge(111) $-$ 2 × 1 surface, Phys. Rev. B **34**, 1330 (1986).

[39] Y. Dorenkamp, H. Y. Jiang, H. Kockert, N. Hertl, M. Kammler, S. M. Janke, A. Kandratsenka, A. M. Wodtke, and O. Bünermann, Hydrogen collisions with transition metal surfaces: Universal electronically nonadiabatic adsorption, J. Chem. Phys. **148**, 034706 (2018).

[40] N. Hertl, K. Krüger, and O. Bünermann, Electronically nonadiabatic H Atom scattering from low Miller index surfaces of silver, Langmuir **38**, 14162 (2022).

[41] K. W. Jacobsen, P. Stoltze, and J. K. Norskov, A semi-empirical effective medium theory for metals and alloys, Surf. Sci. **366**, 394 (1996).

[42] K. W. Jacobsen, J. K. Norskov, and M. J. Puska, Interatomic interactions in the effective-medium theory, Phys. Rev. B **35**, 7423 (1987).

[43] N. Hertl, A. Kandratsenka, and A. M. Wodtke, Effective medium theory for bcc metals: Electronically non-adiabatic H atom scattering in full dimensions, Phys. Chem. Chem. Phys. **24**, 8738 (2022).

[44] M. Kammler, S. M. Janke, A. Kandratsenka, and A. M. Wodtke, Genetic algorithm approach to global optimization of the full-dimensional potential energy surface for hydrogen atom at fcc-metal surfaces, Chem. Phys. Lett. **683**, 286 (2017).

[45] H. C. Andersen, Molecular dynamics simulations at constant pressure and/or temperature, J. Chem. Phys. **72**, 2384 (1980).

[46] T. Yokotsuka, S. Kono, S. Suzuki, and T. Sagawa, Surface electronic structures of Ge(111) surfaces as revealed by temperature dependent UPS, Jpn. J. Appl. Phys. **23**, L69 (1984).

[47] J. Aarts, A. Hoeven, and P. K. Larsen, Core-level study of the phase transition on the Ge(111)-$c(2\times8)$ surface, Phys. Rev. B **38**, 3925 (1988).

[48] K. Hricovini, G. Le Lay, M. Abraham, and J. E. Bonnet, Phase transitions on the Ge(111) and Si(111) surfaces from core-level studies, Phys. Rev. B **41**, 1258 (1990).

[49] L. Pasquali, S. Nannarone, M. Canepa, and L. Mattera, Surface electronic structure of Ge(111) from 300 to 1100 K by metastable deexcitation spectroscopy, Phys. Rev. B **57**, 2507 (1998).

[50] L. Pasquali, S. D'Addato, L. Tagliavini, A. M. Prandini, and S. Nannarone, Surface phase transitions of Ge(111)$c(2\times8)$ studied by electron energy loss spectroscopy, Surf. Sci. **377–379**, 534 (1997).

[51] D. Farias, G. Lange, K. H. Rieder, and J. P. Toennies, Helium scattering structure analyses of the $c(2\times8)$ reconstruction and the high-temperature (1×1) structures of Ge(111), Phys. Rev. B **55**, 7023 (1997).

[52] A. L. Glebov, J. P. Toennies, and S. Vollmer, Behavior of single adatoms on the Ge(111) surface above the 1050 K phase transition, Phys. Rev. Lett. **82**, 3300 (1999).

[53] A. Mak, K. W. Evans-Lutterodt, K. Blum, D. Y. Noh, J. D. Brock, G. A. Held, and R. J. Birgeneau, Synchrotron x-ray diffraction study of the disordering of the Ge(111) surface at high temperatures, Phys. Rev. Lett. **66**, 2002 (1991).

[54] I. A. Vainshtein, A. F. Zatsepin, and V. S. Kortov, Applicability of the empirical Varshni relation for the temperature dependence of the width of the band gap, Phys. Solid State **41**, 905 (1999).